

TNO Defence Research

TNO Physics and Electronics
Laboratory

TD 92-1754

Phone +31 70 326 42 21

TNO-report

copy no.

title

FEL-92-A125

8

First and second order Stokes generation by SRS in methane:
Influence of rep-rate, beam quality and astigmatism

DISTRIBUTION STATEMENT A

Approved for public release;
Distribution Unlimited

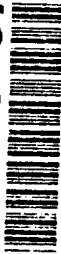
SELECTED
APR 28 1993

author(s):

TDCK RAPPORTCENTRALE

Frederikkazerne, gebouw 140
v/d Burchlaan 31 MPC 16A
TEL. : 070-3166394/6395
FAX. : (31) 070-3166202
Postbus 90701
2509 LS Den Haag

AD-A263 375



TNO Defence Research

TNO Physics and Electronics
Laboratory

Oude Waalsdorperweg 63
2597 AK The Hague
P.O. Box 96864
2509 JG The Hague
The Netherlands

Fax +31 70 328 09 61
Phone +31 70 326 42 21

TNO-report

copy no.

title

FEL-92-A125

8

First and second order Stokes generation by SRS in methane:
Influence of rep-rate, beam quality and astigmatism

DISTRIBUTION STATEMENT A

Approved for public release;
Distribution Unlimited

SELECTED
APR 28 1993
S B D

author(s):

F.J.M. van Putten
J.C. van den Heuvel
R.J.L. Lerou

date:

September 1992

classification

title : unclassified

abstract : unclassified

report text : unclassified

All rights reserved.
No part of this publication may be
reproduced and/or published by print,
photocopy, microfilm or any other means
without the previous written consent of

93-08941



In case this report was drafted on
instructions, the rights and obligations of
contracting parties are subject to either the
'Standard Conditions for Research
Instructions given to TNO', or the relevant
agreement concluded between the
contracting parties.

Submitting the report for inspection to
parties who have a direct interest is
permitted.

TNO

no. of copies : 34

no. of pages : 37 (excluding RDP and distribution list)

no. of appendices : -

All information which is classified according to
Dutch regulations shall be treated by the recipient in
the same way as classified information of
corresponding value in his own country. No part of
this information will be disclosed to any party.

Netherlands organization for
applied scientific research

TNO Defence Research consists of
the TNO Physics and Electronics Laboratory,
the TNO Fluids, Materials Laboratory and the
TNO Chemical Process Laboratory



The Standard Conditions for Research Instructions
given to TNO, as filed at the Registry of the District Court
and the Chamber of Commerce in The Hague
shall apply to all documents supplied to TNO.

93 4 22 008

report no. : FEL-92-A125
title : First and second order Stokes generation by SRS in methane: Influence of rep-rate, beam quality and astigmatism
author(s) : F.J.M. van Putten, J.C. van den Heuvel, R.J.L. Lerou
institute : TNO Physics and Electronics Laboratory
date : September 1992
NDRO no. : A90KL674
no. in pow '92 : -
Research supervised by: R.J.L. Lerou
Research carried out by: F.J.M. van Putten

=====

ABSTRACT (UNCLASSIFIED)

Experiments were performed to obtain a high efficiency for conversion of 1064 nm to eye-safe 1543 nm radiation by stimulated Raman scattering (SRS) in methane.

A first order Stokes photon conversion efficiency of about 75% is obtained for an input energy of 280 mJ, using combinations of cylindrical lenses for focusing. The highest obtainable efficiency appears to be limited by generation of second order Stokes radiation, at a wavelength of 2805 nm.

The energy of the second order Stokes component could be increased to 17.9 mJ, which is sufficient to be useful for medical purposes.

Without circulation of the gas in the Raman cell, thermal blooming effects decreased the efficiency and caused deflection of the beam at pulse repetition rates above 3 Hz. With a gas circulating device, which replaced the gas in the focal area after each laser pulse, we succeeded in maintaining a high efficiency up to 10 Hz (the highest pulse repetition rate of the laser).

This report also includes threshold and beam profile measurements, which were carried out for the evaluation of a numerical model of the stimulated Raman scattering process that is being developed at this laboratory [9].

Beam profile measurements showed that the laser beam can be regarded as "near Gaussian and diffraction limited" only when the smallest available 1.5 mm diaphragm is placed in the laser cavity. With larger laser diaphragms the so called M^2 factor, a parameter describing the quality of the laser beam, must be taken into account. The influence of the beam quality is included in the numerical model and was confirmed by the experimental results.

rapport no. : FEL-92-A125
titel : Opwekking van eerste en tweede orde Stokes d.m.v. SRS in methaan:
Invloed van de puls frequentie, de bundelkwaliteit en astigmatisme.
auteur(s) : ing. F.J.M. van Putten, dr. J.C. van den Heuvel, drs. R.J.L. Lerou
instituut : Fysisch en Elektronisch Laboratorium TNO
datum : september 1992
hdo-opdr.no. : A90KL674
no. in iwp '92 : -
Onderzoek uitgevoerd o.l.v. : R.J.L. Lerou
Onderzoek uitgevoerd door : F.J.M. van Putten

=====

SAMENVATTING (ONGERUBRICEERD)

Dit rapport beschrijft metingen die zijn uitgevoerd met als doel het zo efficiënt mogelijk omzetten van oog-gevaarlijke 1064 nm straling naar oog-veilige 1543 nm straling met gestimuleerde Raman verstrooiing in methaan.

Met combinaties van cilinder lenzen zijn omzettings rendementen van circa 75% gehaald bij een ingangs-energie van 280 mJ. De mogelijkheden tot het halen van een hoger rendement lijken beperkt te worden door omzetting naar tweede orde Stokes straling.

De hoogste energie van de tweede orde Stokes straling, met een golflengte van 2805 nm, was 17.9 mJ. Dit is hoog genoeg om voor medische toepassingen gebruikt te kunnen worden.

Bij een puls frequentie van de laser boven de 3 Hz zonder circulatie van het gas verlaagden thermische effecten in het gas het rendement en veroorzaakten afwijkingen in de bundelrichting. Met een gasverplaatsingssysteem, waarbij na elke laserpuls het gas in het focale gebied vervangen wordt, was er geen invloed meer van de puls frequentie op het rendement tot en met 10 Hz (de hoogste puls frequentie van de laser).

Ter evaluatie van een theoretische model van gestimuleerde Raman verstrooiing dat op dit laboratorium wordt ontwikkeld [9], zijn "threshold" metingen en bundelprofiel metingen verricht.

Uit de bundelprofiel metingen bleek dat de bundel alleen als "gaussisch en diffractie begrensd" beschouwd kan worden als het kleinste 1.5 mm diafragma in de lasercavity wordt geplaatst. Bij grotere diafragma's moet rekening gehouden worden met de zgn. M^2 -factor, een parameter die de kwaliteit van de laserbundel beschrijft. Experimenten bevestigen de invloed van de bundelkwaliteit, zoals in het numerieke model wordt voorspeld.

ABSTRACT	2
SAMENVATTING	3
CONTENTS	4
1 INTRODUCTION	5
2 FIRST ORDER STOKES	6
2.1 SRS with astigmatic foci	6
2.2 Experimental set-up for SRS	7
2.3 Results for several optical configurations	9
2.4 Conclusions	13
3 SECOND ORDER STOKES	15
3.1 Cascade stimulated Raman scattering	15
3.2 Detection of second order Stokes	15
3.3 Second order Stokes generation	16
3.4 Conclusions	18
4 BEAM QUALITY MEASUREMENTS	19
4.1 Laser beam characterization	19
4.2 The M^2 factor	19
4.3 Beam quality measurement techniques	20
4.4 Beam quality for several laser configurations	22
4.5 Conclusions	25
5 THRESHOLD MEASUREMENTS	27
5.1 Low power SRS	27
5.2 Detection of radiation at low output energies	30
5.3 Thresholds with spherical and astigmatic foci	30
5.4 Conclusions	33
6 CONCLUSIONS	34
7 LITERATURE	36

Earlier experiments [1] showed deflection and distortion of the laser beam at rep-rates above 3 Hz due to thermal blooming effects in the gas. These alterations of the beam shape and direction were measured with a 32 X 32 pyro-electric detector array (Spiricon, Inc.) at 1064 nm, 1543 nm (first Stokes) and at 2805 nm (second Stokes) at low and high rep-rates.

Accession For

NTIS GRA&I	<input checked="checked" type="checkbox"/>
DTIC TAB	<input type="checkbox"/>
Unannounced	<input type="checkbox"/>
Justification	

By _____

DTIC Accession # _____

Availability Codes

Availability Codes

Dist. _____

A-1

2 FIRST ORDER STOKES

2.1 SRS with astigmatic foci

The first experiments with astigmatic foci were done with two uncoated cylindrical lenses, placed in such a way that they give a focal area of two ellipses, with perpendicular main axes, a distance ΔF apart (fig. 1).

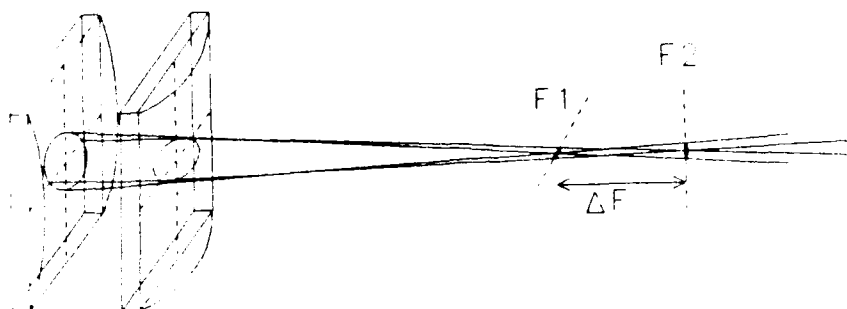


Fig. 1: Focal area with cylindrical lenses

By varying the ΔF and the focal lengths of the lenses, the focal area of lens combinations can be optimized in order to obtain the highest conversion efficiency that is possible at a given pulse energy and beam diameter.

The new anti-reflection-coated cylindrical lenses have focal lengths of 80, 100, 125 and 150 mm. The ΔF 's were varied from 13 mm to 28 mm.

Beside reaching a high conversion efficiency, the experiments are aimed at maintaining this efficiency at high rep-rates.

The Nd:YAG laser (BMI D.NS.501) can work at rep-rates up to 10 Hz. Earlier experiments [1] gave a large decrease in conversion efficiency at rep-rates above 3 Hz.

After each laser pulse, focused in the Raman cell, a part of the pulse energy is transferred to the methane in the focal area [1]. It is assumed this causes thermal blooming effects in the gas, resulting in a decrease in the output energy and deflection and distortion of the laser beam. In order to circumvent these effects, mechanical devices were tested to circulate the methane in the focal region.

2.2 Experimental set-up for SRS

The experimental set-up for the SRS measurements is shown in figure 2.

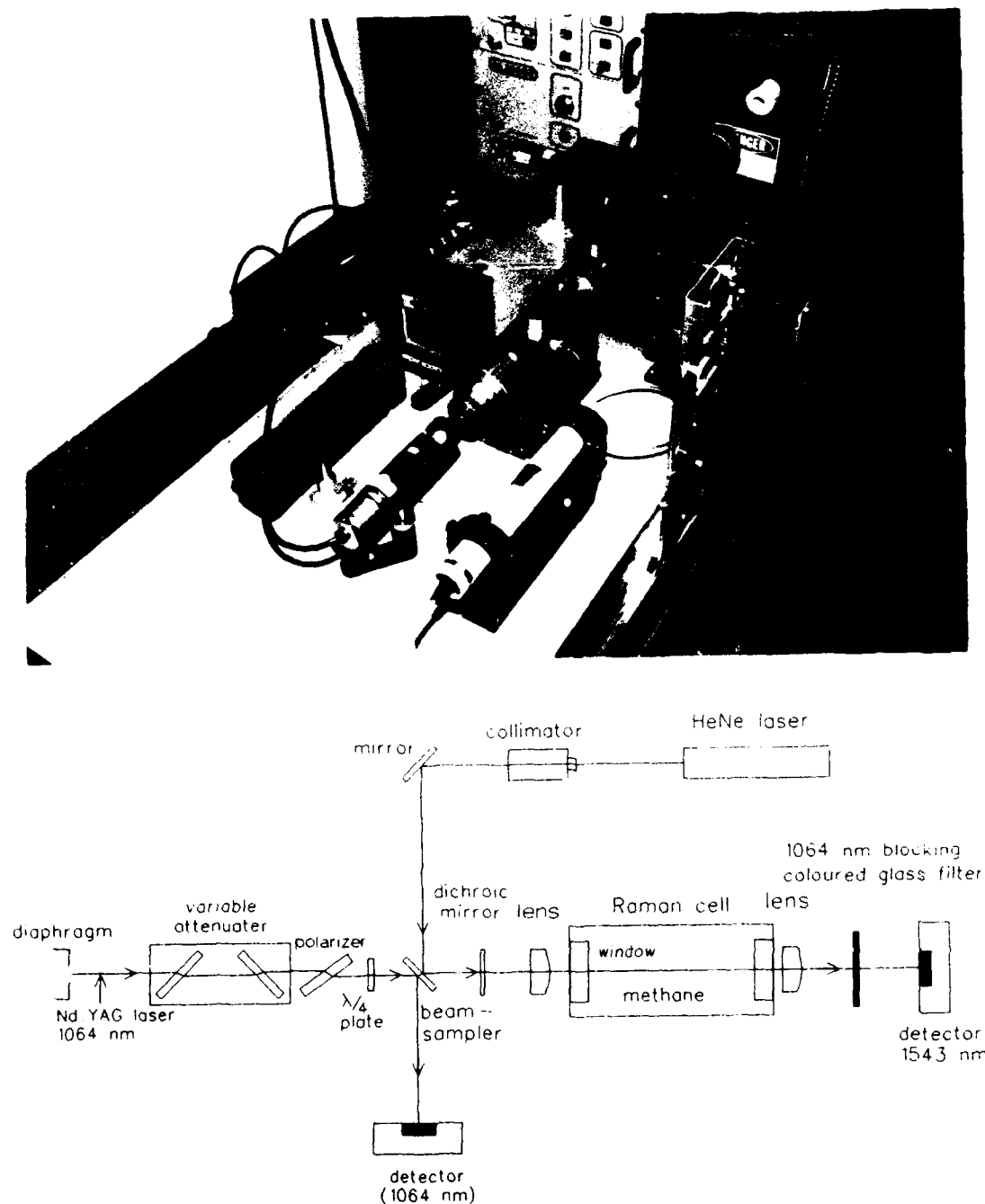


Fig. 2: Set-up for SRS measurements

The Nd:YAG laser beam is focused into the Raman cell, containing methane under high pressure (90 bar). A dichroic mirror, transmitting at 1064 nm and reflecting at 1543 nm, reflects the backward scattered 1543 nm radiation back into the Raman cell. The backwards scattered energy, which would otherwise be lost, now contributes to the total forward going energy and gives an extra stimulation of the conversion process.

The pulse energy of the 1543 nm radiation is measured behind a coloured glass filter (BG 38) at the exit of the Raman cell. The photon quantum conversion efficiency η is then calculated with corrections for reflection losses at the optics of the Raman cell and the photon energy:

$$\eta = \frac{E_{\text{srs}}}{E_{\text{YAG}}} \cdot \frac{1.543}{1.064} \cdot \frac{1}{T_{\text{cell}}} \quad (1)$$

E_{srs} : energy at 1543 nm (J)

E_{YAG} : energy pump beam (J)

T_{cell} : transmission Raman cell (%)

Diaphragms in the laser cavity, with diameters ranging from 1.5 mm to 6.5 mm, are used to change the beam diameter and the maximum pulse energy. For the measurements with the 6.5 mm diaphragm, a lens with a focal length of 2 m was placed near the laser, to decrease the beam diameter at the entrance of the Raman cell. Without this lens the beam would be too large to pass through the cell.

More details about the set-up are given in the previous report [1].

At high rep-rates without proper measures the efficiency drops considerably [1].

In order to avoid the decrease in the conversion efficiency at high rep-rates, a piezo-electric driven blade was placed near the focal area of the lens inside the Raman cell, as shown in figure 3.

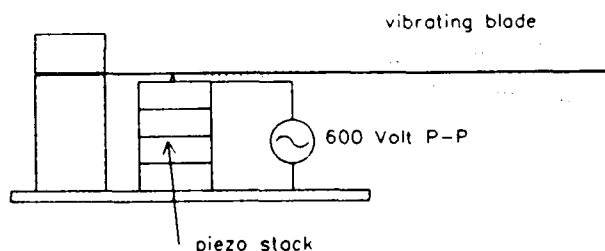


Fig. 3: Vibrating blade in Raman cell

By applying the resonance frequency of the blade to the piezo-electric element, the amplitude of the vibrating blade can be maximized to provide a maximal mechanical stirring of the gas.

A more controllable method is shown in figure 4. A revolving partitioned cylinder (RPC) is placed inside the Raman cell.

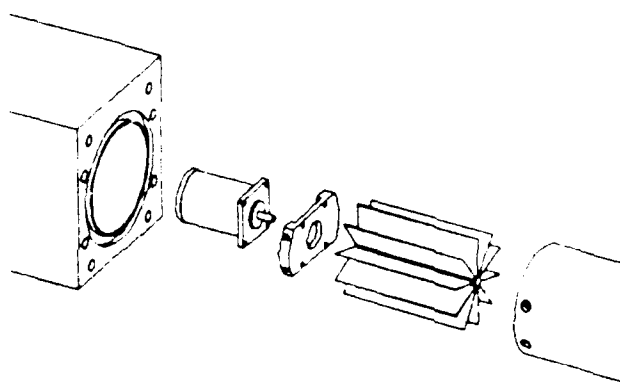


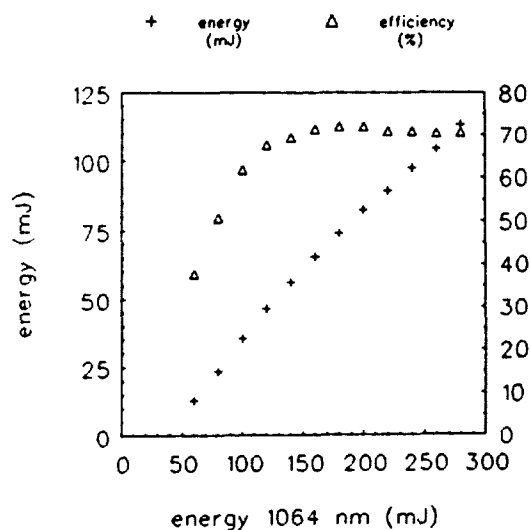
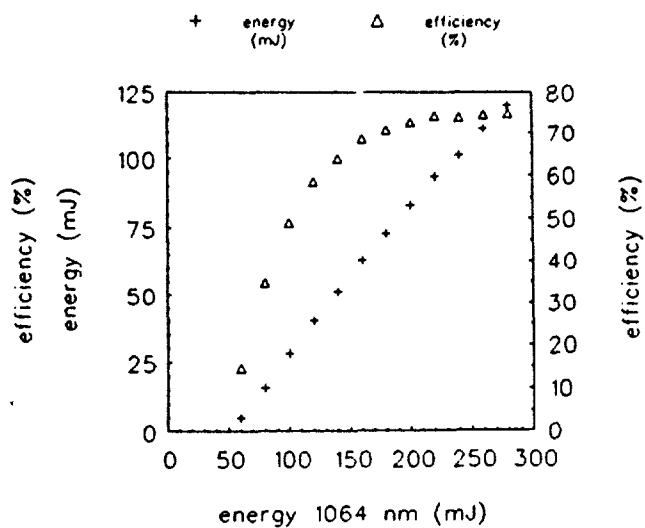
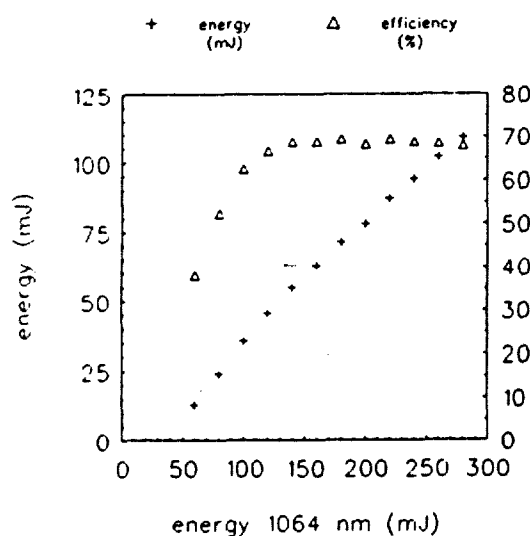
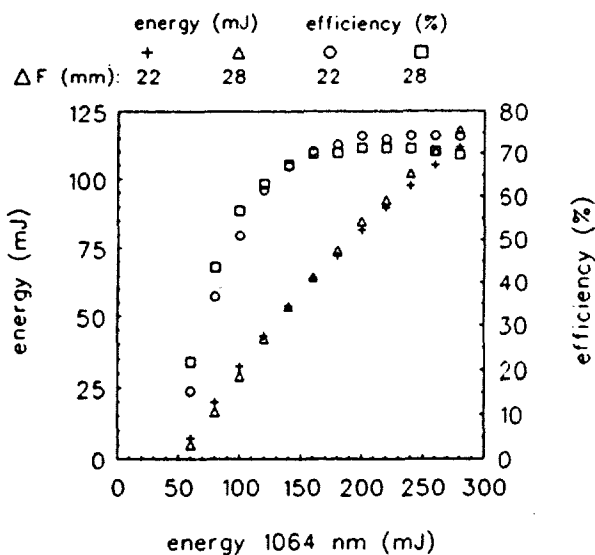
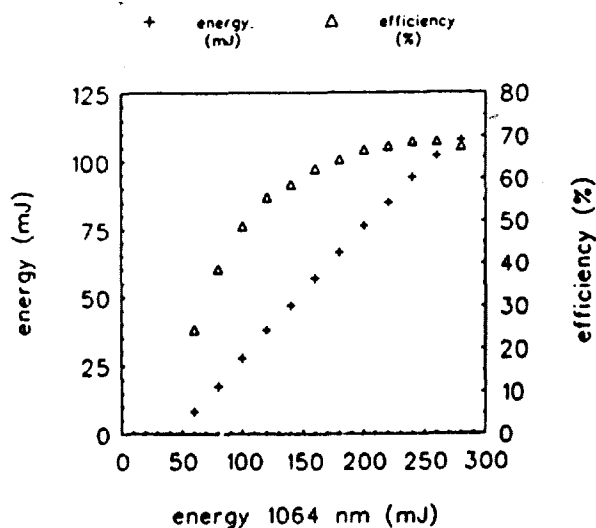
Fig. 4: SRS with an RPC in the Raman cell

This RPC is a cylinder with a diameter of 30 mm, divided in ten separate compartments. After every laser pulse the cylinder is rotated by a stepper motor. The next laser pulse is focused into the next compartment filled with methane, recovered from the previous laser pulses. Earlier experiments [1] showed no influence of the rep-rate at 1 Hz. At a rep-rate of 10 Hz the rep-rate inside each of the 10 compartments is also 1 Hz. Thus, when the laser is working at 10 Hz, there should not be an influence of the rep-rate on the efficiency or the beam properties.

2.3 Results for several optical configurations

2.3.1 Low rep-rate pump

Measurements were done with cylindrical lens combinations of 150/125, 150/100, 125/125, 125/100 and 100/100 mm with different ΔF 's at high pulse energies with the largest laser diaphragm of 6.5 mm, which resulted in a maximum input pulse energy of about 300 mJ. The results of these measurements are shown in fig. 5, 6, 7, 8 and 9, where the photon conversion efficiency and the energy of the 1543 nm pulse is given as a function of the input pulse energy.

Fig. 5: SRS with F=150/125 mm and $\Delta F=22$ mmFig. 6: SRS with F=150/100 mm and $\Delta F=28$ mmFig. 7: SRS with F=125/125 mm and $\Delta F=13$ mmFig. 8: SRS with F=125/100 mm and $\Delta F=22$ and 28 mmFig. 9: SRS with F=100/100 mm and $\Delta F=13$ mm

The highest conversion efficiency was about 75%, obtained with the 150/100 mm lens combination with a ΔF of 37 mm at an input pulse energy of 280 mJ.

This is about the same as the earlier reported results [1] with uncoated lenses. The increase of transmission of the optics seems to have little effect on the photon conversion efficiency. Note that optical losses are compensated for in the calculation of the efficiency.

The use of uncoated optics between the focus and the dichroic mirror reduces the stimulation of the SRS process due to the reflection of the backwards scattered radiation. The fact that the use of AR-coated lenses did not result in an increase of the highest obtained photon conversion efficiency may be caused by an increase of second Stokes generation at the expense of the first Stokes component.

Having lower reflection losses results in an increase of the output energy at 1543 nm. The maximal obtained energy at 1543 nm at the exit of the Raman cell with an input energy of 250 mJ is 105 mJ. Earlier we reported, with the same input energy, an output energy of 77 mJ [1]. When the input energy was increased to 280 mJ, the output energy at 1543 nm with AR-coated lenses could be increased to 120 mJ, as shown in fig. 6.

2.3.2 Conversion at high rep-rates

To avoid the influence of thermal blooming in the gas at high rep-rates two mechanical gas circulation devices are tested.

The first attempts of reducing thermal blooming effects at high rep-rates were performed with a vibrating blade in the Raman cell (fig. 3). By changing the frequency of the piezo element driver, the output power of 1543 nm radiation was optimized at the frequency where the blade was vibrating at its resonance frequency.

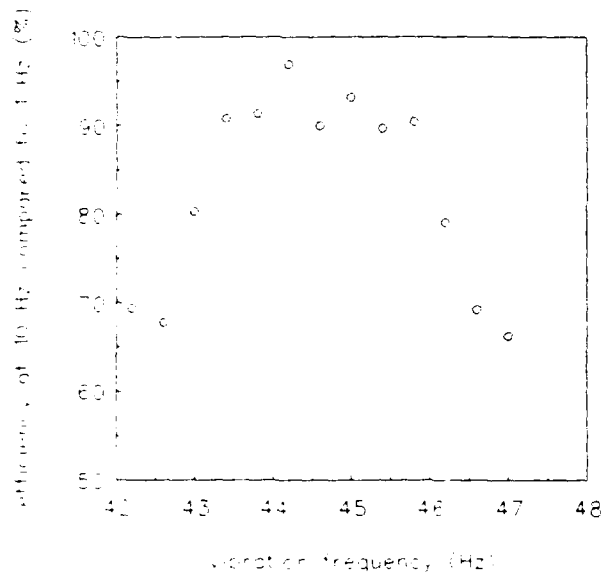


Fig. 10: Efficiency as a function of vibration frequency

Figure 10 shows to which level the output power of the first Stokes at 10 Hz rep-rate can be restored compared to the output at a low rep-rate (the efficiency at 1 Hz is taken as 100%).

However, this result could not be reproduced at later experiments, when the vibrating blade did not have any effect on the conversion efficiency. Therefore we tried a different method.

The RPC (fig. 4) was more effective than the vibrating blade. The efficiency of the conversion process could be maintained up to 10 Hz at the same level as at low rep-rates (fig. 11).

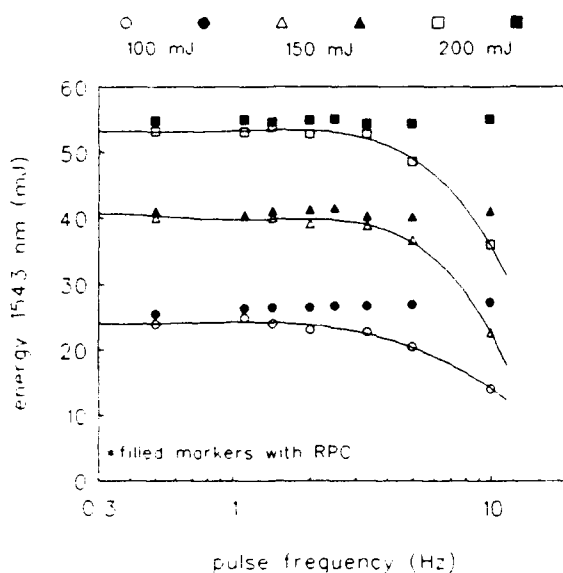


Fig. 11: Effect of the RPC on the efficiency

This figure shows the earlier results [1], and the results after the installation of the RPC.

Because the maximal rep-rate of the laser is 10 Hz the RPC could not be tested at higher rep-rates. Without the RPC the rep-rate must not be higher than 2 Hz [1]. If the maximal rep-rate is 2 Hz for each of the 10 compartments of the RPC a maximal rep-rate of about 20 Hz must be feasible. To be able to work with rep-rates above 20 Hz an RPC with more compartments is required.

2.4 Conclusions

The highest obtained output energy at 1543 nm is 120 mJ, which is a quantum conversion efficiency of about 75%. This is about the same efficiency as earlier reported with uncoated cylindrical lenses [1], so that the increase of transmission of the optics seems to have little effect on the photon conversion efficiency. This is most likely caused by an increase of second Stokes generation at the expense of the first Stokes component. However, because of the lower reflection losses at the optics than at the earlier experiments [1] the output energy that can be obtained is significantly higher.

The method of decreasing the effect of thermal blooming with a vibrating blade appears to be very critical and difficult to reproduce.

A revolving partitioned cylinder (RPC) is an efficient method of gas circulation. With this device high efficiency SRS is possible with high rep-rate lasers. Due to the maximal rep-rate of the laser the performance could not be tested above 10 Hz, but higher rep-rates up to about 20 Hz should be possible.

3 SECOND ORDER STOKES

3.1 Cascade stimulated Raman scattering

For the generation of 1543 nm radiation the dichroic mirror must be set in the position which gives the highest efficiency of the SRS process. As was reported earlier [1] the optimal position of the mirror was not perpendicular to the laser beam but, contrary to what was expected, at a slight angle. It was concluded that this was due to cascade Raman scattering, i.e. conversion by SRS from 1543 nm to 2805 nm, giving a high amount of second order Stokes radiation at 2805 nm.

Therefore, the generation of second order Stokes has been investigated.

Because of the low penetration depth in water there is also an interest for radiation at this wavelength for medical purposes [2][3]. To be useful for surgery for e.g. the cornea the pulse energy should reach values of about 10 mJ with a rep-rate above 10 Hz [2].

3.2 Detection of second order Stokes

The BK7 windows of the Raman cell do not transmit radiation with a wavelength above 2300 nm. For the measurement of the second order Stokes component of 2805 nm the window at the exit of the cell is replaced by a CaF_2 window, which transmits radiation up to 9000 nm.

To protect a long pass filter from high intensity radiation the output pulse is first attenuated by reflection on a prism. With this long pass filter (2300 nm), blocking the 1064 nm and the 1543 nm radiation, only the second Stokes component is measured, see fig. 12.

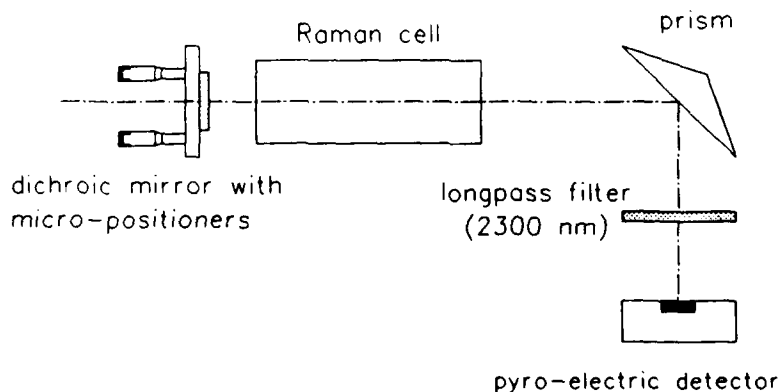


Fig. 12: Set-up for second Stokes measurements

3.3 Second order Stokes generation

The second order Stokes appeared to be very sensitive to the dichroic mirror alignment. Fig. 13 shows the first and second Stokes component as a function of x-value of the micropositioner of the dichroic mirror holder.

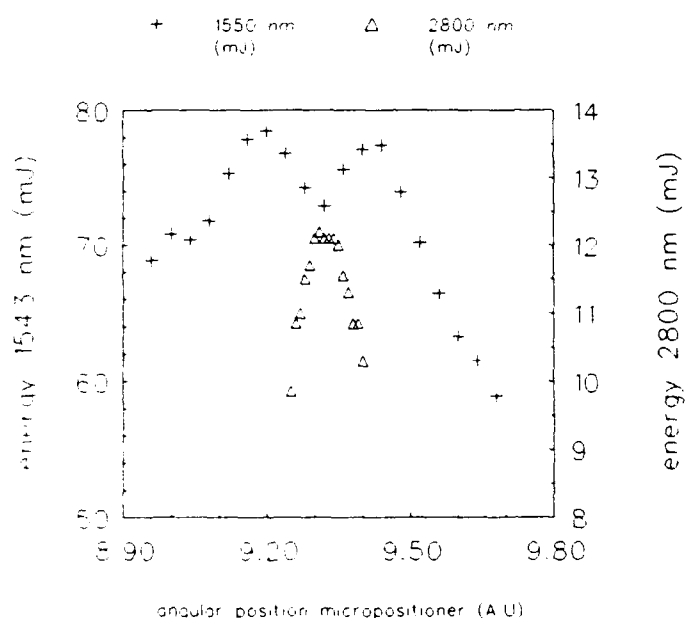


Fig. 13: First and second order Stokes components as a function of alignment of the dichroic mirror.

The first Stokes component shows a decrease where the second Stokes is maximal. For second Stokes generation, the best x-position of the dichroic mirror is where there is a local minimum in the first Stokes output due to cascade SRS. This results in a considerable increase in 2805 nm radiation.

This was repeated for the y-value of the micropositioner of the mirror holder, showing the same effect.

The generation of second Stokes radiation was measured with spherical lenses and with combination of cylindrical lenses. In fig. 14 the results with spherical lenses ($F=100$ and 125 mm) are shown.

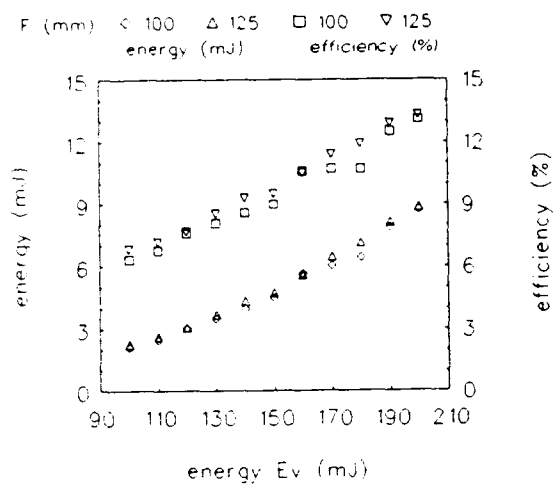


Fig. 14: Second Stokes SRS with spherical lenses

With the following combinations of cylindrical lenses, $F=125/125$ mm with a ΔF of 10 mm and $F=100/100$ mm with a ΔF of 13 mm, the amount of second Stokes generation could be increased, to 17.9 mJ.

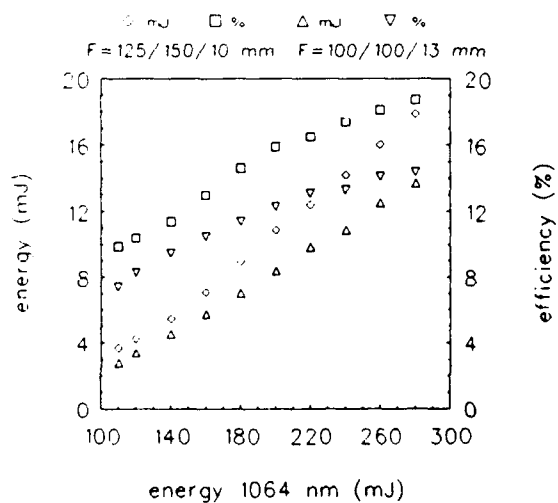


Fig. 15: Second Stokes SRS with cylindrical lenses

With the help of a *dichroic mirror*, that also reflects 2805 nm, the amount of 2805 nm radiation may increase. However, the needed triple wavelength AR-coating for this set-up consists of a large number of layers, reducing the damage threshold to an unpractically low level. Therefore it is necessary to use uncoated CaF_2 optics at the entrance of the Raman cell. This results in reflection losses of about 6% per element, which has a large effect on the output of the second Stokes component.

3.4 Conclusions

The second order Stokes component obtains a maximum at the position where there is a local minimum in the first Stokes component. The conclusion that the decrease in the first Stokes is due to second order Stokes generation [1] appears to be valid.

The energy needed for medical purposes is about 10 mJ [2]. With our set-up this can be reached at a input of about 200 mJ.

4 BEAM QUALITY MEASUREMENTS

4.1 Laser beam characterization

For a better understanding of the SRS measurements the intensity profile and the propagating of the laser beam were measured, as well in the focal area as of the unfocused beam.

The beam intensity profiles of the Nd:YAG laser, the 1543 nm and the 2805 nm radiation were measured with the pyro electric detector array of a beam profiler (Spiricon, Inc.), both at low and at high rep-rates. These measurements give an indication of the beam profile and show effects causing beam distortion, e.g. thermal blooming.

However, a profiler, fixed at one point in the beam, has difficulty revealing the contents of the different modes in the multimode mixture of a non-diffraction limited laser beam.

The multimode beam has an increased beam divergence, which can be measured with the knife edge-method [5][6]. This method is used to measure the diameter of the laser beam at the dichroic mirror position, at the entrance of a large focal length lens ($F=700$ mm) and in the focal area. With these results the beam quality is calculated, compared to gaussian beam performance. This can be expressed by a parameter, M^2 [5], describing the quality of the laser beam.

4.2 The M^2 factor

To characterize several non-gaussian multi-mode laser beams, a measurable parameter, M^2 [5], can be used. The M^2 factor is the product of the beam's minimum diameter and divergence angle, normalized to the fundamental (TEM_{00}) mode value [5]:

$$M^2 = \frac{\pi}{4} \theta \frac{2w_0}{\lambda} \quad (2)$$

θ : full-angle divergence (rad)

w_0 : waist radius (m)

λ : wavelength (m)

As can be seen, when the beam is gaussian TEM_{00} with $\theta=2\lambda w_0 / \pi$, then $M^2 = 1$.

If this parameter is known, the theory for calculations with gaussian beams can be applied after a minor adaption. By measuring the spot diameter of a laser beam with known diameter, focused with an aberration free lens, the M^2 factor can be calculated [5]

$$w(z) = w_0 \sqrt{1 + \left(\frac{M^2 \lambda z}{w_0^2 \pi} \right)^2} \quad (3)$$

$w(z)$: waist radius at distance Z (m)

Z : distance lens from focus (m)

This can also be written as

$$M^2 = \frac{w_0 \pi}{\lambda z} \sqrt{w(z)^2 - w_0^2} \quad (4)$$

Equation (4) is used to measure the M^2 factor for a number of laser beams.

4.3 Beam quality measurement techniques

4.3.1 Beam profiler

The Spiricon beam profiler consists of an array (32 X 32) of pyro-electric detectors, forming a sensitive square area of 25 cm². In the experiments the laser or Stokes beam is expanded by a beam-expander (5X) and then detected by the array (see fig. 16).

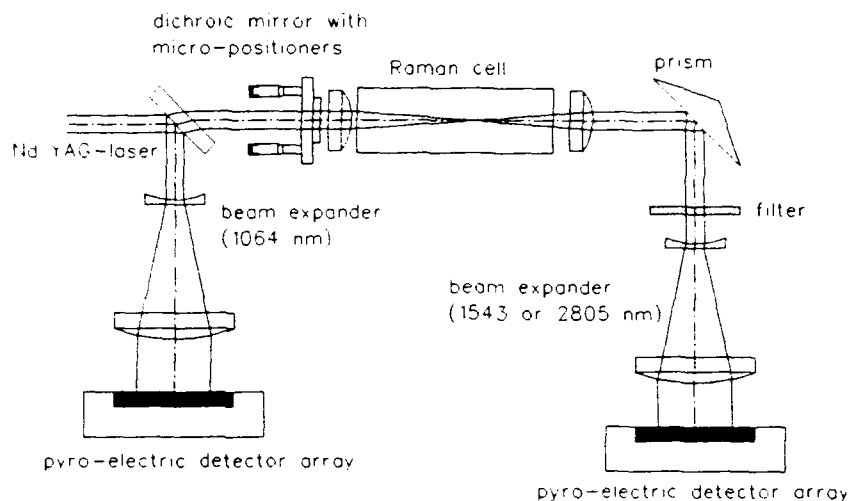


Fig. 16: Beam profile measurements with detector array

The results can be averaged by the Spiricon software, which can also perform a gaussian fit of the data. From this fit the correlation factor between a perfect gaussian profile and the measured profile can be calculated. A correlation factor of 1 means that the beam profile is a perfect gaussian.

4.3.2 Knife-edge

With the knife-edge technique a sharp black piece of metal is placed on an x-translation stage and is moved with small steps across the attenuated beam (Fig. 17).

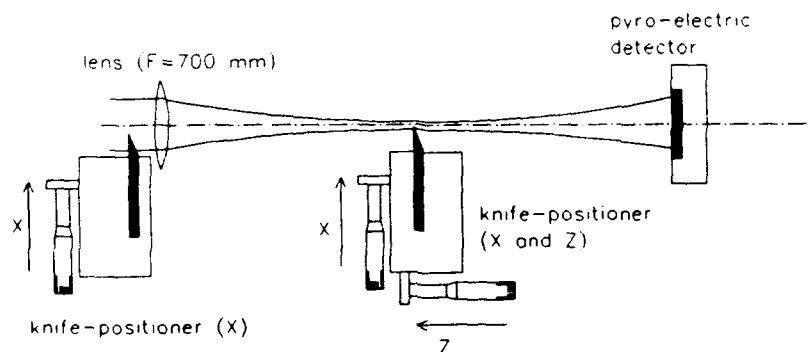


Fig. 17: Beam width measurement with knife-edge technique

The energy of the pulse that is not blocked by the knife is measured by a detector. By measuring the energy passing the knife as a function of the knife position, we find an S-curve, from which the beam diameter can be calculated [8].

In [6] it is suggested to take the positions where between 10% and 90% of the energy passes the knife and to use an additional scale factor to calculate the beam width. For these knife positions the error in beam width is minimized for the different possible modes in the laser beam. However, here the positions where 16% and 84% of the energy reaches the detector are taken as the half beam width. Although this is only exact when the beam is gaussian [6], these clip-levels increase the experimental accuracy, since at low energy levels the positioning of the knife is less accurate.

4.4 Beam quality for several laser configurations

4.4.1 Beam profiler measurements

In fig. 18 and 19 the expanded beam is shown, as measured with the detector array, for the 1.5 mm and the 6.5 mm diaphragm, respectively. The correlation factor between a perfect gaussian beam profile and the measured profiles, calculated by the Spiricon software, was 0.977 for the 1.5 mm and 0.979 for the 6.5 mm diaphragm, suggesting that the beams are fairly gaussian shaped.

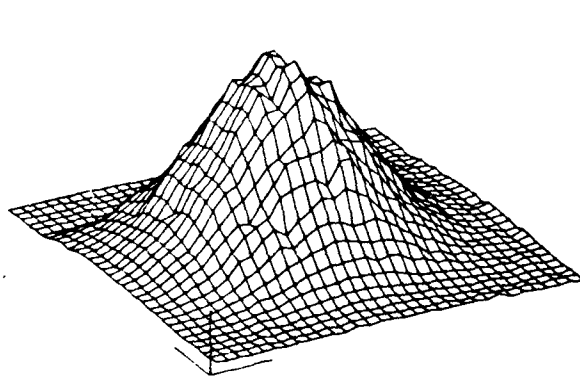


Fig. 18: Beam profile with 1.5 mm diaphragm

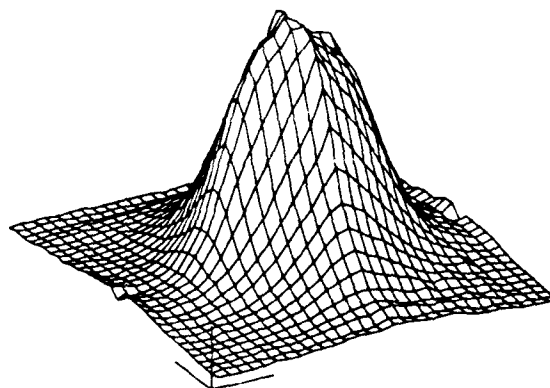


Fig. 19: Beam profile with 6.5 mm diaphragm

The generation of first order Stokes at a low frequency (1 Hz) is shown in figure 20.

At 10 Hz (fig. 21), without gas circulation, the effects of thermal blooming in the focal area are very clear.

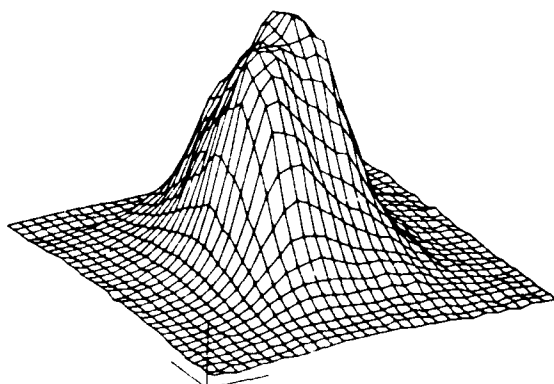


Fig.20: First Stokes component at low rep-rate (1 Hz)

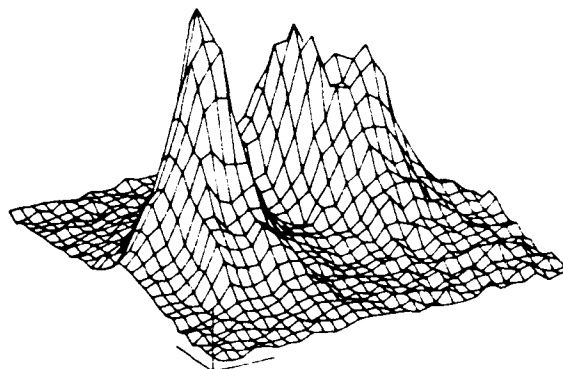


Fig.21: First Stokes component at high rep-rate without recirculation (10 Hz)

The beam shows high intensity peaks and is largely distorted. The same effect can be seen in the second order Stokes profile measurements (fig. 22 and fig. 23).

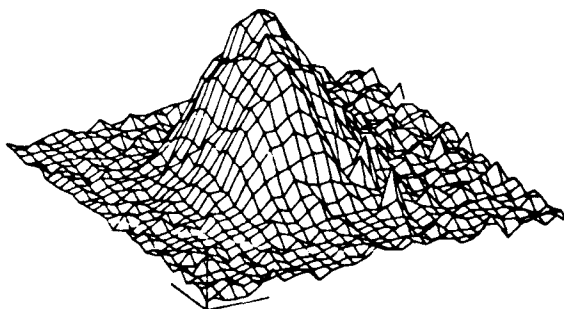


Fig.22: Second Stokes component at low rep-rate (1 Hz)

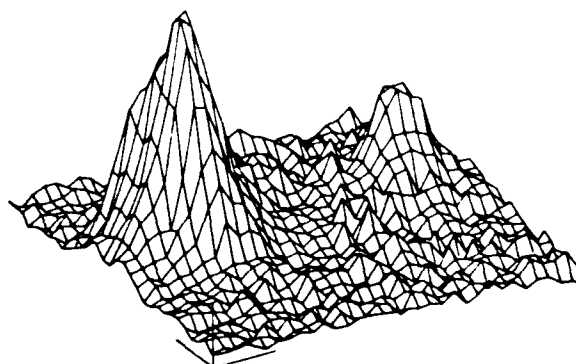


Fig.23: Second Stokes component at high rep-rate without recirculation (10 Hz)

For high rep-rates, this set-up is not suitable and an effective gas circulation device is required. No beam profile measurements have been done with the RPC (fig.4) yet, but efficiency measurements showed that thermal blooming effects in the focus have been avoided (fig. 11).

4.4.2 Knife-edge measurements

The S-curves of the laser beam are measured with the knife-edge method for laser diaphragms with the following diameters: 1.5 mm, 2 mm and 6.5 mm. The knife was placed successively at the normal dichroic mirror position, at the entrance of a large focal length lens and in the focus of that lens.

In fig. 24 and 25 the results of the measurements of the 1.5 mm diaphragm is given, for the unfocused (at lens position) and the focused laser beam.

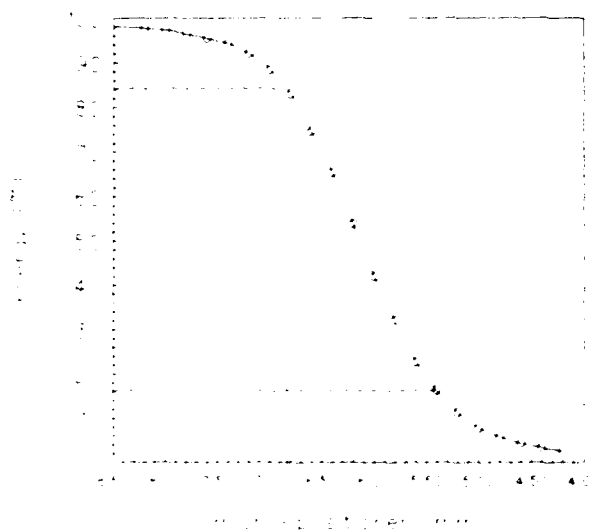


Fig. 24: S-curve of laser beam at lens position

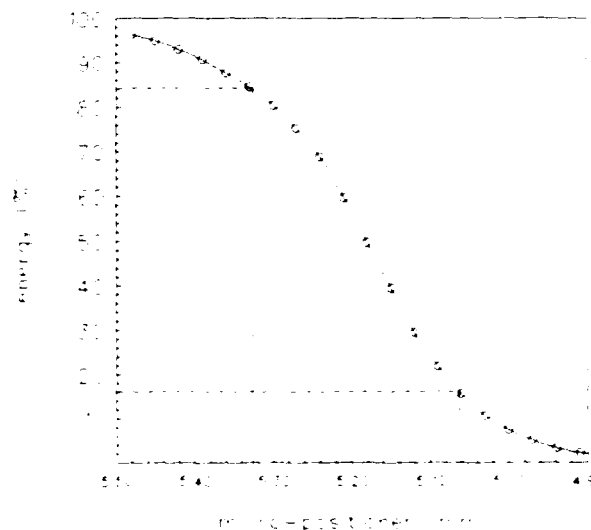


Fig. 25: S-curve at focus of laser beam

The diameter at the dichroic mirror position, calculated from the 16% and 84% energy points was 2.40 mm, at the lens position it was 2.85 mm.

After focusing with a $F=700$ mm lens, the smallest beam width was found at a distance of 95.5 cm and was 0.516 mm (fig. 25). This closely matches the expected focal diameter of a gaussian beam ($2w_0=0.453$ mm), resulting in $M^2=1.12$, using equation (4).

With the 6.5 mm laser diaphragm the laser beam was collimated with a weak lens ($F=2$ m, [1]), before focusing with the lens with a focal length of 700 mm.

The results of the measurements of the S-curve of the collimated laser beam and of it's focus are shown in fig. 26 and fig.27.

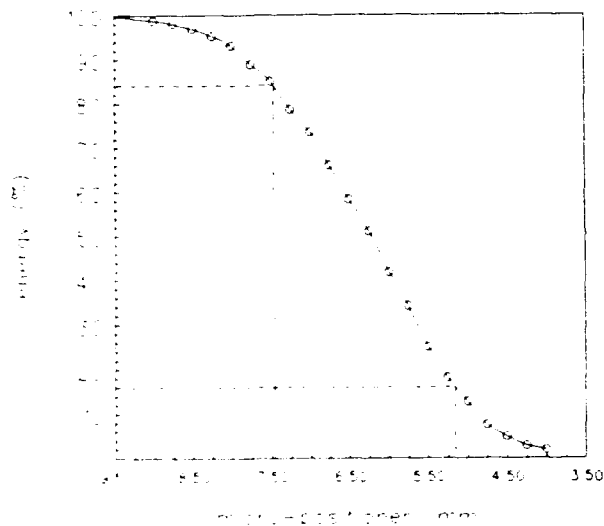


Fig. 26: S-curve of laser beam at lens position

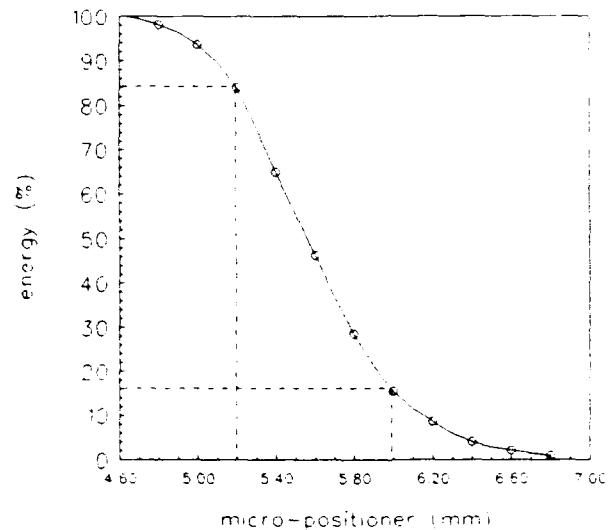


Fig. 27: S-curve at focus of laser beam

The beam diameter at the dichroic mirror position, calculated from the 16% and 84% energy points was 5.7 mm, and at the entrance of the lens 4.60 mm. The diameter of the focus, at 56.5 cm from the lens (the beam is slightly convergent due to the $F=2$ m lens, which places the focus closer to the lens than its focal length) was 1.57 mm. This is much larger than the focus of a TEM_{00} diffraction limited gaussian beam with the same diameter, which gives a diameter at the focus of 0.166 mm. The M^2 factor was here calculated to be 8.9 (eq. 4).

The same measurements were done with the 2 mm diaphragm, which resulted in a M^2 of 1.8. The small increase of the diameter of the diaphragm in the laser cavity from 1.5 mm to 2.0 mm is already sufficient to give a large increase in the M^2 factor.

4.5 Conclusions

For numerical simulations the beam quality factor M^2 must be taken into account.

Although the Spiricon beam profiler seems to indicate that the beam profile is fairly gaussian shaped, it is obvious from knife-edge measurements, that at high pulse energies, when the largest laser diaphragm of 6.5 mm is used, the beam can not be regarded as a single mode TEM_{00} gaussian beam. With this 6.5 mm diaphragm the M^2 factor was calculated to be 8.9. With this laser the beam can be regarded as "near gaussian and diffraction limited", only when the smallest diaphragm of 1.5 mm is used, resulting in an M^2 factor of 1.12.

The influence of thermal blooming in the gas on the propagation of the first and second order Stokes beam at a high rep-rate can be made visible with the beam profiler. For determining the beam quality factor M^2 , the knife-edge method is a more appropriate tool.

5 THRESHOLD MEASUREMENTS

5.1 Low power SRS

The threshold energy for the stimulated Raman process gives information about the energy which is needed in a particular optical configuration to start the conversion process. Threshold measurements have also been very useful for the evaluation of the theoretical model, under development by van den Heuvel [4][9].

Parameters which can have a large effect at high pulse energies (e.g. stimulated Brillouin scattering and ground state depletion) have not been included in the theoretical model, yet [9]. These effects are not likely to play an important role at the low pulse energy where the threshold measurements are done.

What is regarded as the threshold energy is usually the minimal detectable energy, which depends on the specifications of the detectors used [7,p.303]. A more practical value for the threshold energy is the 1% conversion efficiency limit [8].

Because the SRS process occurs when the laser pulse power is at it's highest level, the time dependence of the pulse shape must be taken into account. This time dependence is shown in figure 28.

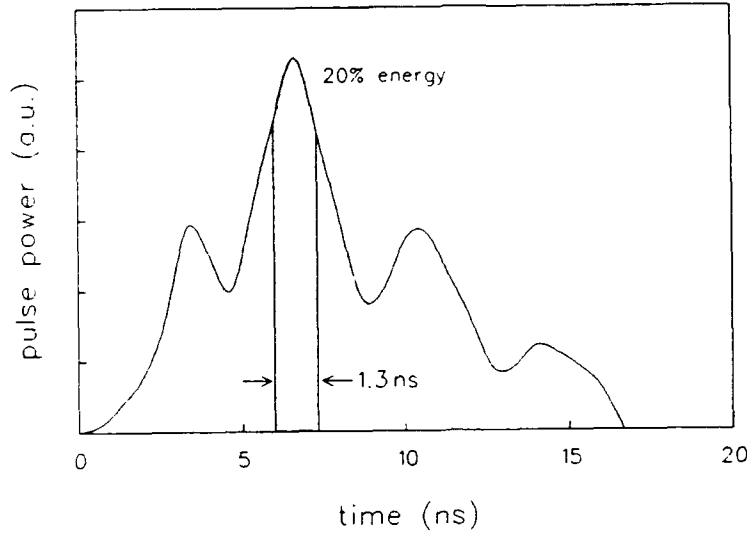


Fig. 28: Digitized oscilloscope trace of the laser pulse

The area with the highest peak power, about 1.3 ns long, contains about 20% of the total pulse energy. Only the peak power will contribute to the Stokes pulse, so the threshold level is the pulse energy where the conversion efficiency is 0.2%.

Because the Raman gain coefficient has been measured by others [8], we can compare the measured threshold energy with the calculated threshold energy in the numerical model, using this gain coefficient.

The amplification, or gain, is defined as:

$$G = \ln \frac{E_{s(\text{exit})}}{E_{s(\text{entrance})}} \quad (5)$$

$E_{s(\text{exit})}$: energy stokes at exit cell (J)

$E_{s(\text{entrance})}$: energy stokes at entrance cell (J)

The threshold energy is defined by the requirement that the Stokes gain is e^{25} , thus when $G=25$.

A simple analytical model gives for the amplification at threshold energy [8]

$$G = g P_p \frac{\pi n}{\lambda} \quad (6)$$

g : Raman gain coefficient (m/W)

P_p : power pump beam (W)

n : index of refraction of methane

The threshold power, as follows from equations (5) and (6) and $G=25$, is given by

$$P_p = \frac{25\lambda}{\pi n g} \quad (7)$$

The detectors measure the pulse energy and not the pulse power. By assuming that the Stokes energy is only generated in the pulse peak of 1.3 ns width containing 20% of the total pulse energy, as shown in figure 28, we can calculate the energy E_p in this part of the laser pulse with the highest power

$$E_p = P_p \cdot 1,3 \times 10^{-9} \cdot 5 \quad (8)$$

This gives for the threshold energy (7)(8)

$$E_p = \frac{1,63 \times 10^{-7} \lambda}{\pi n g} \quad (9)$$

When the beam is not a single mode gaussian ($M^2 > 1$) [9]

$$E_p = 1,63 \times 10^{-7} \frac{M^2 \lambda}{\pi n g} \quad (10)$$

5.2 Detection of radiation at low output energies

Measurements of the threshold energy are almost the same as normal SRS efficiency measurements, except that they are done at a low pulse energy without the dichroic mirror (Fig. 2).

The result is a very low output of 1543 nm radiation with a large spread in energy. To get reliable results, pulse energies are averaged over typically two or three hundred laser pulses.

5.3 Thresholds with spherical and astigmatic foci

In fig. 29 the results of the threshold measurements are given for the smallest laser diaphragm (1.5 mm) with two spherical lenses: $F=100$ and 125 mm.

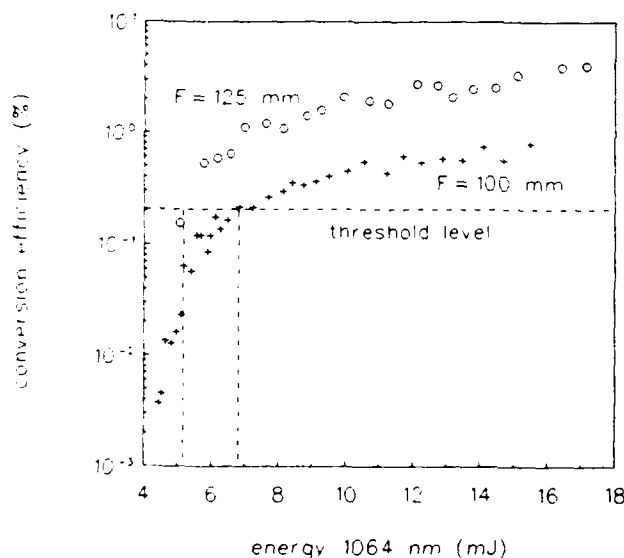


Fig. 29: Threshold energy for spherical lenses

The measured threshold energies at 0.2% conversion efficiency are 6.85 mJ at $F=100$ mm and 5.20 mJ at $F=125$ mm. The measured threshold energies can be compared with the theoretical results of equation (10). The calculated threshold energy here is 12.1 mJ, using equation (10) with $M^2=1.12$, $n=1.04$ and $g=0.49 \cdot 10^{-9}$ cm/W.

The results of measurements of threshold energies with the 1.5 mm diaphragm and combinations of cylindrical lenses with different ΔF 's are shown in fig. 30 and 31.

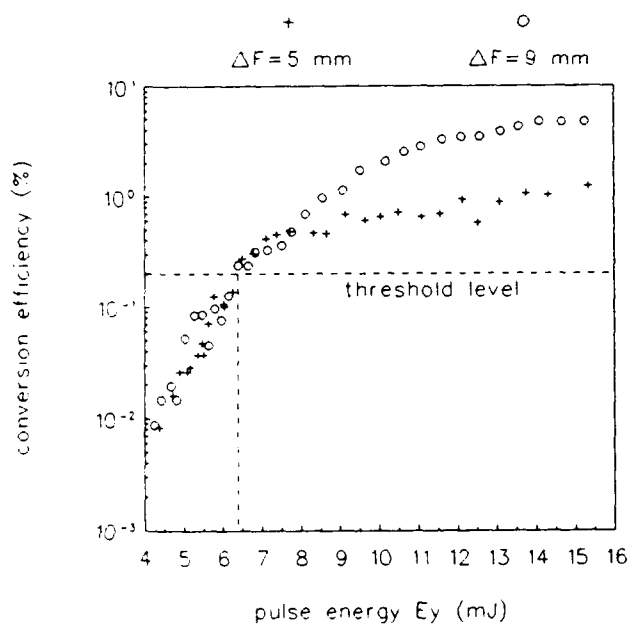


Fig.30: Threshold energy with cylindrical lenses

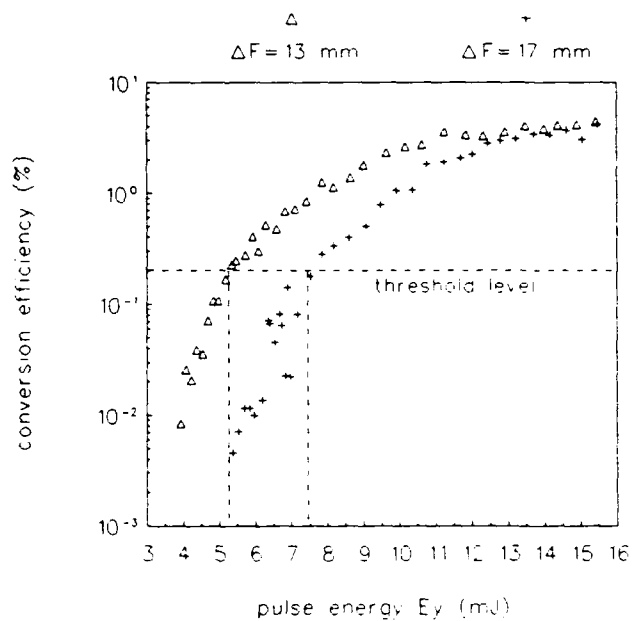


Fig.31: Threshold energy with cylindrical lenses

For the 6.5 mm laser diaphragm, threshold energies were found to be much higher (fig. 32), ranging from 37.5 mJ with the $F=100$ mm lens to 47 mJ with the $F=150$ mm lens. This could be expected due to the large M^2 -factor that was found, which gives a much lower intensity in the focal region. The calculated threshold energy for this M^2 (8.9), using equation (10), is 96 mJ.

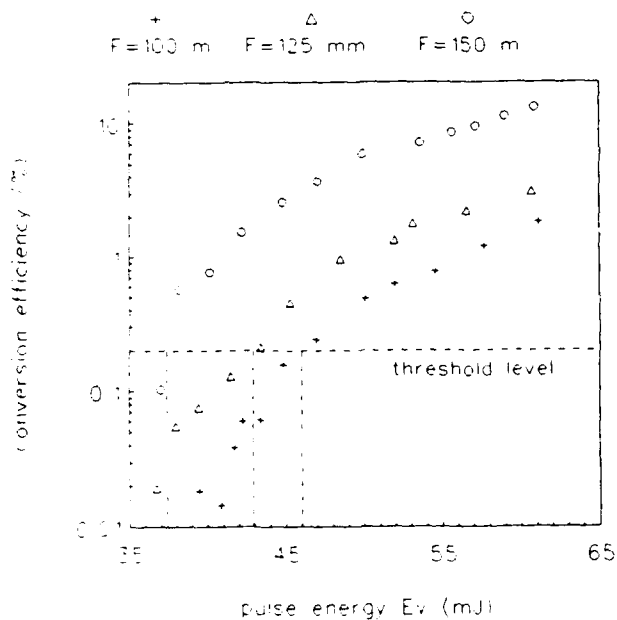


Fig.32: Threshold energy with spherical lenses

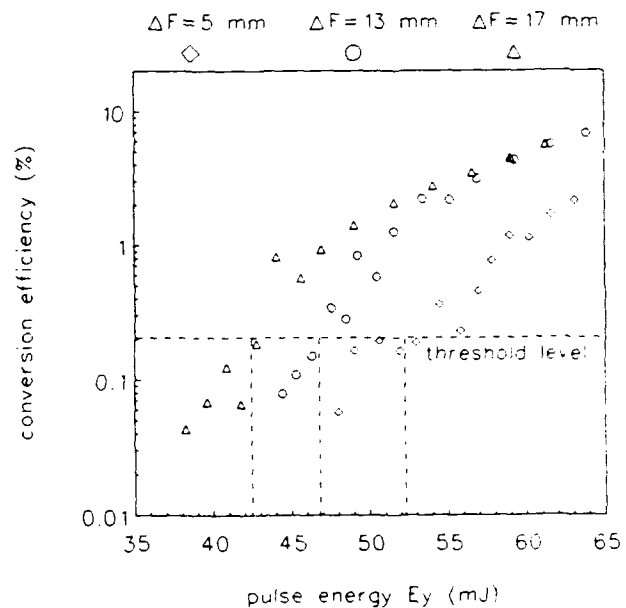


Fig.33: Threshold energy with cylindrical lenses

Threshold energies with combinations of cylindrical lenses are shown in Fig. 33 for 3 ΔF 's. An increase in the ΔF gives a higher threshold, as is also found in the numerical model [4].

The results from equation (10) give about a factor 2 higher threshold energies than the measurements. However, this equation is derived from a simple model which does not include important factors, like gain focusing and reflections from the cell windows [4]. In the numerical model of J.C. van den Heuvel [9], which includes these effects, the measurements and the calculated results as shown in fig. 34 are in good agreement.

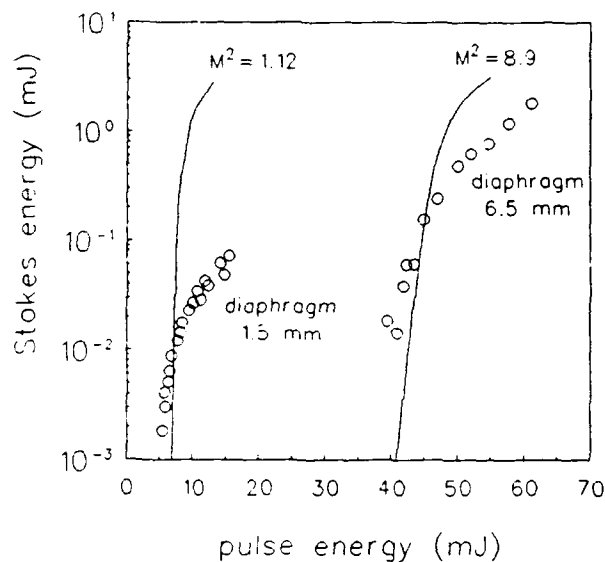


Fig. 34: Comparison numerical model and experimental results

5.4 Conclusions

The threshold measurements, with information of the beam quality (M^2 -factor), supply useful information for the evaluation of the numerical model that is under development by J.C. van den Heuvel [9].

The measured threshold energies are lower than the calculated values of the analytical model. In the calculations of this simple analytical model important effects, such as gain focusing and reflection from the cell windows [4], have not been taken into account. For the numerical model, which include these effects, the experimental results agree well with the calculated values [9].

6 CONCLUSIONS

With combinations of cylindrical lenses, the SRS process in methane can convert eye hazardous 1064 nm to eye-safe 1543 nm radiation with a high conversion efficiency. The highest conversion efficiency of about 75% was obtained with 2 cylindrical lenses with focal lengths of 150 mm and 100 mm, placed so that ΔF is 28 mm.

A higher efficiency appears not easily possible due to the increased generation of second order Stokes radiation at 2805 nm at the expense of the 1543 nm energy.

The highest output at 1543 nm that was reached was 120 mJ with a input energy at 1064 nm of 280 mJ. In other words, an energy conversion of more than 40%, including reflecting losses in the Raman cell, has been obtained.

Beam profile measurements with a detector array showed a large distortion of the beam shape at high rep-rates as a result of thermal blooming effects. For high rep-rates a gas circulating device is necessary.

Attempts with a piezo-electric driven vibrating blade stirring the gas, to suppress thermal blooming, were not reproducible. However, a revolving partitioned cylinder (RPC), placed inside the Raman cell, succeeded in maintaining a high conversion efficiency up to 10 Hz, the maximal rep-rate of the laser.

Earlier results [1] showed no effect of the rep-rate up to about 3 Hz without a gas circulation device. If the maximal rep-rate can be increased up to 2 pulses for each of the 10 compartments, the highest rep-rate which would give good results in our set-up would be about 20 Hz.

The generation of second order Stokes radiation can be increased to a conversion efficiency of 17.5%, which corresponds to 17.9 mJ at an input of 280 mJ. This was obtained with a combination of 2 cylindrical lenses with focal lengths of 150 mm and 125 mm, placed so that ΔF is 10 mm. This output is significant enough to explain the observed decrease of the energy of the first Stokes component at high input levels.

As is reported [2] an output energy of more than 10 mJ is high enough to be useful for medical purposes. In our set-up this can be obtained at an input energy of about 200 mJ.

Beam profile measurements, with a detector array and with the knife-edge method, showed that the laser beam can be regarded as "near gaussian and diffraction limited" only when the smallest diaphragm, being 1.5 mm, is placed in the laser cavity.

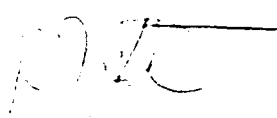
In that case an M^2 of 1.12 is found. With a 2 mm diaphragm the M^2 increases to 1.8, and with the 6.5 mm diaphragm an M^2 of 8.9 is found.

The results of threshold measurements, combined with the M^2 factor measurements, showed a good agreement with the calculated results from a numerical model that is under development at this laboratory by J.C. van den Heuvel [9].

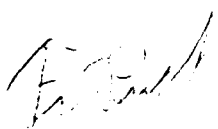
7 LITERATURE

- [1] F.J.M. van Putten,
'Opwekking van hoogvermogen 1.54 μm straling m.b.v. gestimuleerde Raman verstrooiing in methaan'.
Fysisch en Electronisch Laboratorium,
TNO report.: FEL-90-B098, 1990.
- [2] C. Gunterman, V. Schultz-von der Gathen and H.V. Döbele,
'Raman shifting of Nd:YAG laser radiation methane: an efficient method to generate 3- μm radiation for medical uses',
Applied Optics 28, 135-138 (1989).
- [3] H.J. Eichler, H. Meng, M. Glotz, and J. Chen,
'Effective generation of 3 μm pulsed radiation by raman scattering in a capillary',
Optics communications 77 (1990), pp 80-84.
- [4] J.C. van den Heuvel,
'Numerical modeling of stimulated raman scattering in an astigmatic focus',
IEEE Journal of Quantum Electronics, vol. 28, pp. 378-385, 1992.
- [5] T.F. Johnsen Jr.,
'M² concept characterizes beam quality',
Laser Focus world, pp. 173-183, may 1991.
- [6] A.E. Siegman, M.W. Sasnett, and T.F. Johnsen Jr.,
'Choice of clip levels for beam width measurements using knife-edge techniques',
IEEE Journal of Quantum Electronics, vol. 27, pp. 1098-1104, 1991.
- [7] A. Anderson,
'The raman effect (1,2)',
Marcel Dekker, Inc., New York 1971 (1973).

- [8] D.C. Hanna, D.J. Pointer and D.J. Pratt,
'Stimulated raman scattering of picosecond light pulses in hydrogen, deuterium and methane',
IEEE Journal of Quantum Electronics, vol. 22, pp. 332-336, 1986
- [9] J.C. van den Heuvel, F.J.M. van Putten, and R.J.L. Lerou,
'The stimulated raman scattering threshold for a nondiffraction-limited pump beam',
To be published in the september issue of the IEEE Journal of Quantum Electronics



R.J.L. Lerou
(group leader)



F J M. van Putten
(author)

REPORT DOCUMENTATION PAGE

(MOD-NL)

1. DEFENSE REPORT NUMBER (MOD-NL)	2. RECIPIENT'S ACCESSION NUMBER	3. PERFORMING ORGANIZATION REPORT NUMBER
TD92-1754		FEL-92-A125
4. PROJECT/TASK/WORK UNIT NO.	5. CONTRACT NUMBER	6. REPORT DATE
22459	A90KL674	SEPTEMBER 1992
7. NUMBER OF PAGES	8. NUMBER OF REFERENCES	9. TYPE OF REPORT AND DATES COVERED
37 (EXCL. RDP. EXCL. DISTRIBUTION LIST)	9	FINAL REPORT
10. TITLE AND SUBTITLE FIRST AND SECOND ORDER STOKES GENERATION BY SRS IN METHANE: INFLUENCE OF REP-RATE, BEAM QUALITY AND ASTIGMATISM		
11. AUTHOR(S) F.J.M. VAN PUTTEN, J.C. VAN DEN HEUVEL AND R.J.L. LEROU		
12. PERFORMING ORGANIZATION NAME(S) AND ADDRESS(ES) TNO PHYSICS AND ELECTRONICS LABORATORY, P.O. BOX 96864, 2509 JG THE HAGUE OUDE WAALSDORPERWEG 63, THE HAGUE, THE NETHERLANDS		
13. SPONSORING/MONITORING AGENCY NAME(S)		
14. SUPPLEMENTARY NOTES		
15. ABSTRACT (MAXIMUM 200 WORDS, 1044 POSITIONS) Experiments were performed to obtain a high efficiency for conversion of 1064 nm to eye-safe 1543 nm radiation by stimulated Raman scattering (SRS) in methane. A first order Stokes photon conversion efficiency of about 75% is obtained for an input energy of 280 mJ, using combinations of cylindrical lenses for focusing. The highest obtainable efficiency appears to be limited by generation of second order Stokes radiation, at a wavelength of 2805 nm. The energy of the second order Stokes component could be increased to 17.9 mJ, which is sufficient to be useful for medical purposes Without circulation of the gas in the Raman cell, thermal blooming effects decreased the efficiency and caused deflection of the beam at pulse repetition rates above 3 Hz. With a gas circulating device, which replaced the gas in the focal area after each laser pulse, we succeeded in maintaining a high efficiency up to 10 Hz (the highest pulse repetition rate of the laser). This report also includes threshold and beam profile measurements, which were carried out for the evaluation of a numerical model of the stimulated Raman scattering process that is being developed at this laboratory (9). Beam profile measurements showed that the laser beam can be regarded as "near Gaussian and diffraction limited" only when the smallest available 1.5 mm diaphragm is placed in the laser cavity. With larger laser diaphragms the so called M^2 factor, a parameter describing the quality of the laser beam, must be taken into account. The influence of the beam quality is included in the numerical model and was confirmed by the experimental results.		
16. DESCRIPTORS LASERS RAMAN SCATTERING CONVERSION EYESAFE-LASERS	IDENTIFIERS METHANE ND-YAG STIMULATED RAMAN SCATTERING	
17a. SECURITY CLASSIFICATION (OF REPORT) UNCLASSIFIED	17b. SECURITY CLASSIFICATION (OF PAGE) UNCLASSIFIED	17c. SECURITY CLASSIFICATION (OF ABSTRACT) UNCLASSIFIED
18. DISTRIBUTION/AVAILABILITY STATEMENT NO RESTRICTIONS	17d. SECURITY CLASSIFICATION (OF TITLES) UNCLASSIFIED	